J Am Soc Nephrol 11: 270–282, 2000

Nephrocystin: Gene Expression and Sequence Conservation between Human, Mouse, and *Caenorhabditis Elegans*

EDGAR OTTO,* ANDREAS KISPERT,† SILVIA SCHÄTZLE,* BIRGIT LESCHER,† CORNELIA RENSING,* and FRIEDHELM HILDEBRANDT*

**University Children's Hospital, Freiburg University, and †Max-Planck Institute for Immunobiology, Freiburg, Germany.*

Abstract. Juvenile nephronophthisis, an autosomal recessive cystic kidney disease, is the primary genetic cause for chronic renal failure in children. The gene (*NPHP1*) for nephronophthisis type 1 has recently been identified. Its gene product, nephrocystin, is a novel protein of unknown function, which contains a *src*-homology 3 domain. To study tissue expression and analyze amino acid sequence conservation of nephrocystin, the full-length murine *Nphp1* cDNA sequence was obtained and Northern and *in situ* hybridization analyses were performed for extensive expression studies. The results demonstrate widespread but relatively weak *NPHP1* expression in the human adult. In the adult mouse there is strong expression in testis. This expression occurs specifically in cell stages of the first meiotic division and thereafter. *In situ* hybridization to whole mouse embryos demonstrated widespread and uniform expression at all developmental stages. Amino acid sequence conservation studies in human, mouse, and *Caenorhabditis elegans* show that in nephrocystin the *src*-homology 3 domain is embedded in a novel context of other putative domains of protein-protein interaction, such as coiled-coil and E-rich domains. It is concluded that for multiple putative protein-protein interaction domains of nephrocystin, sequence conservation dates back at least to *Caenorhabditis elegans*. The previously described discrepancy between widespread tissue expression and the restriction of symptoms to the kidney has now been confirmed by an in-depth expression study.

Juvenile nephronophthisis (NPH), an autosomal recessive cystic kidney disease, is the primary genetic cause for chronic renal failure in children (1–3). NPH shows a characteristic pattern of renal histology, which consists of tubular basement disintegration, interstitial cell infiltration, tubular atrophy, and cyst formation (4). A group of diseases exhibiting renal histology identical to NPH is summarized under the term nephronophthisis/medullary cystic disease (NPH/MCD) complex.

Disruption of several unlinked genes leads to this renal histopathologic picture. In recessive NPH, at least three different gene loci are known. The gene (*NPHP1*) responsible for juvenile nephronophthisis (NPH1; MIM 256100) is localized on human chromosome 2q12-q13 (5,6). A gene locus for infantile nephronophthisis (*NPH2*; MIM 602088) is localized on chromosome 9q22-q31 (7), and a third gene locus for adolescent nephronophthisis (*NPH3*) has been mapped to chromosome 3q21-q22 (H. Omran, C. Fernandez, M. Jung, K. Häffner, B. Fargier, A. Villaquira, R. Waldherr, N. Gretz, M. Brandis, F. Rüschendorf, A. Reis, F. Hildebrandt. Identification of a new gene locus for adolescent nephronophthisis on chromosome 3q22 in a large Venezuelan pedigree, submitted for publication). In addition, recessive forms of NPH with extrarenal involvement are known. In Senior-Løken syndrome (8), NPH is associated with retinitis pigmentosa (MIM 266900) (9), and in Cogan syndrome NPH occurs in combination with oculomotor apraxia (10). Autosomal dominant forms of the NPH/MCD complex lead to end-stage renal failure only in the third decade of life or later and are not associated with extrarenal manifestations (11). For these disease variants, the term "autosomal dominant medullary cystic kidney disease (ADMCKD)" is used. A gene locus for ADMCKD1 (MIM 174000) has been localized to chromosome 1q21 (12). A second locus was mapped to chromosome 16p12 (13), and the existence of a third locus has been suggested (A. Fuchshuber, personal communication).

Very little is known about the pathogenesis of NPH. As a first step in its analysis, we have recently identified by a positional cloning approach the gene for juvenile nephronophthisis type 1 (5). This gene (*NPHP1*) encodes a novel gene product termed nephrocystin, which contains a *src*-homology 3 (SH3) domain. SH3 domains are modular protein-binding domains and are known to interact strongly with proteins, which contain a proline-rich recognition sequence of the consensus "PXXP" and are found in focal adhesion signaling complexes (14,15). To date, few data are available on the expression pattern of the *NPHP1* transcript, as well as on structural motifs and evolutionary conservation of its gene product nephrocystin.

We have previously identified several alternative splice variants of *NPHP1* (5). *NPHP1* exon 9 possesses a unique strong splice acceptor for different alternative weak splice donors of

Received June 29, 1999. Accepted July 31, 1999.
Correspondence to Dr. Friedhelm Hildebrandt, University Children's Hospital, Mathildenstrasse 1, D-79106, Freiburg, Germany. Phone: +49 761 270 4301; Fax: +49 761 270 4533; E-mail: hildebra@kkl200.ukl.uni-freiburg.de
1046-6673/1102-0270
Journal of the American Society of Nephrology

exon 8. The weak splice donors of exon 8 may be read through to produce a short 5′ transcript of *NPHP1*.

To study evolutionary sequence conservation of *NPHP1*, in this study we obtained full-length cDNA sequence of the mouse homologue and identified a *Caenorhabditis elegans* (*C. elegans*) homologue in a database search. Nephrocystin exhibits an evolutionary conserved and hitherto unknown association of an SH3 domain with other putative domains of protein-protein interaction, such as coiled-coil and E-rich domains.

Expression analysis of human mRNA revealed widespread but weak tissue distribution. In the adult mouse there is very strong expression in testis. *In situ* hybridization analysis reveals that this expression occurs specifically in cell stages of the first meiotic division and thereafter. *In situ* hybridization to whole mouse embryos demonstrates widespread and uniform expression at all developmental stages. These data provide the first evidence that nephrocystin is highly conserved between a wide range of species, and might be an important constituent of a majority of cells in the body. Prominent expression in adult testis of the mouse suggests a role in sperm cell differentiation.

Materials and Methods

Southern Blotting

A Southern blot of *Eco*RI-digested genomic DNA of nine different species was probed with a human *NPHP1* cDNA clone containing sequence from exon 10 to the end of the coding region (nucleotides [nt] 1022–2138). The blot was washed at normal stringency and signals were detected by autoradiography, according to a standard protocol (16).

cDNA Library Screening and cDNA Sequencing

About 1×10^6 plaques of a mouse diaphragm cDNA library (no. 937393; Stratagene, Heidelberg, Germany), constructed with a Uni-ZAP-XR phage vector, were screened by hybridization with mouse 3′ EST clone vg40 h08 at normal stringency according to the manufacturer's protocol. This clone covers the sequence from exon 18 to the end of the coding region (nt 1794–2235). Briefly, the EST fragment was P^{32}-labeled by random prime labeling (Amersham, Braunschweig, Germany). Transformants were replicated onto Hybond N^+ filters (Amersham) and hybridized overnight at 60°C in 20 ml of ExpressHyb™ hybridization solution (Clontech, Palo Alto, CA). Filter membranes were washed for 10 min with 2× SSC buffer and 0.05% sodium dodecyl sulfate at room temperature and exposed to x-ray film with two intensifying screens for 16 h. The only positive cDNA clone MD1 was plaque-purified, subcloned into pBluescript SK+ (Stratagene), and directly sequenced by fluorescently labeled dideoxy sequencing, using T3 and T7 primers on an ABI 377 Sequencer (Applied Biosystems, Foster City, CA).

Rapid Amplification of cDNA Ends and PCR

To obtain full length of the mouse *Nphp1* transcript, 5′ rapid amplification of cDNA ends (RACE) was carried out using a mouse testis Marathon™ cDNA amplification kit according to the manufacturer's protocol (no. 7413-1; Clontech). To obtain clone M-a, primary and nested PCR were carried out using primers from adaptor AP1 with mouse-specific primer (derived from clone MD1) MD1–596− (5′-TCAACTCCTTCAGCATCCTTAGCCAGCC-3′), and in a subsequent nested PCR with adaptor AP2 and internal primer MD1–505− (5′-CCAGTCTGCTGAGCAGCGAAGTCCCC-3′). A similar protocol was applied to generate the murine partial cDNA clone M1357–1774, using primers MD1–1357+ (5′-GGTGACTGTTTTATCAGGTCC-3′); and MD1–1774− (5′-CATCTCCAAGAATTTGTCGG-3′), which were derived from mouse cDNA clone MD1.

Northern Blot Analysis

A normalized human poly(A)$^+$RNA dot blot (no. 7770-1; Clontech) containing 43 different human adult and seven fetal tissues, and a murine poly(A)$^+$RNA dot blot (no. 7771-1; Clontech) containing 18 murine adult and four fetal tissues were hybridized with *Nphp1* cDNA probes according to standard (16) and the manufacturer's protocol. Probes used were a 3′-specific human *NPHP1* cDNA containing exons 9 to 20 (nt 1026–2114), a 5′-specific human cDNA containing exons 1 to 8 (nt 10–937), and murine *Nphp1* cDNA clone MD1 containing exons 5 to 20 without exons 14 to 16 (nt 456-2217). (All positions are given in relation to the human start codon.) Optical density was normalized against the background signal on 100 ng of yeast and *Escherichia coli* RNA and expressed as relative units.

A multiple tissue Northern blot with human adult poly(A)$^+$RNA (MTN7760-1; Clontech) was hybridized at normal stringency with a 5′-specific human cDNA, which contains exons 1 to 8 only (nt 10–937). Standard (16) and the manufacturer's protocols were applied. A multiple tissue Northern blot containing 20 μg of murine poly(A)$^+$RNA was hybridized at normal stringency with mouse *Nphp1* cDNA clone MD1 (nt 465-2217) as described previously (17). Exposure for autoradiography was 3 wk.

In Situ Hybridization

Antisense *Nphp1* cDNA from murine clone MD52-2284 was hybridized to whole mouse embryos and to tissue sections of murine adult testis. Clone MD52-2284 was constructed by PCR using clones M-a and MD1 as templates with primers MD52+ (5′-GCAGGAGCTGAAGCTGCAG-3′) and MD2284− (5′-GCATATGACTACGTTCTAACC-3′). This clone encompasses murine *Nphp1* sequence, which is equivalent to human exons 1 to 20 without exons 14 to 16. Sense sequence was used as negative control. The protocol used for whole-mount *in situ* hybridization is based on a procedure described by Parr *et al.* (18) and was modified according to Knecht *et al.* (19). *In situ* hybridization on tissue sections was carried out according to Lescher *et al.* (20) with the following modification: Prehybridization and hybridization were carried out at 70°C. After the hybridization, all steps followed the procedure described for whole-mount *in situ* hybridization.

Sequence Data

The composite human cDNA *NPHP1* sequence is from GenBank (accession nos. AF023674 and AJ001815). Here we use the sequence of AF023674, based on clone EO3, which codes for two glutamine residues at positions 313 and 314, whereas AJ001815 codes for only one glutamine residue. The cDNA sequence of the *C. elegans NPHP1*-like sequence was derived from genomic sequence generated by the Sanger Center (GenBank accession no. Z49911), and from EST clone yk467b4.5. The sequence of the full-length murine *Nphp1* cDNA isolated in this study was deposited with GenBank (accession no. AF127180).

Statistical Analyses

For cDNA and amino acid sequence comparisons, the following programs from the Genetics Computer Group (GCG) Wisconsin were run at the Heidelberg Unix Sequence Analysis Resources (HUSAR) (URL: http://genius.embnet.dkfz-heidelberg.de:8080/): BLAST,

PILEUP, and CLUSTAL. Standard parameters were applied. Figure 1 was produced using the programs LINEUP and PRETTYBOX. The secondary structure prediction program COILS was run at the Baylor College of Medicine site (URL: http://dot.imgen.bcm.tmc.edu:9331/).

Results

Sequence Conservation of NPHP1

To evaluate sequence conservation of *NPHP1*, a Southern blot of genomic DNA from nine different species was hybridized with a human 1116-bp probe representing *NPHP1* cDNA sequence from exon 10 to the end of the coding region. Recognition of 1 to 5 bands in each lane indicated sequence conservation of the *NPHP1* gene in mammals (Figure 2). This probe does not contain the SH3 domain. No bands were detected in chick and yeast. Rehybridization with a 5′ probe encoding the SH3 domain yielded a single band also in yeast and chick (data not shown).

Isolation of Murine Nphp1 cDNA

To generate additional data on *NPHP1* sequence conservation and splicing patterns, and to be able to compare tissue expression patterns between human and mouse, we isolated murine *Nphp1* cDNA. Because *NPHP1* expression was previously found to be strongest in skeletal muscle (5), a murine diaphragm cDNA library (no. 937393; Stratagene) was screened at 10^6 recombinants with mouse 3′ EST vg40 h08, which shows sequence similarity to human *NPHP1* cDNA from exon 18 to the end of the coding region. Only one positive clone was isolated. This cDNA clone, termed MD1 (Figure 3g), was sequenced from both strands. Because MD1 was incomplete at its 5′ end, RACE on murine testis cDNA (no. 7455-1; Clontech) was performed, extending available sequence information 70 nucleotides 5′ beyond the putative start codon in human (clone M-a) (Figure 1, Figure 3i).

Within human exon 8, murine clone MD1 was colinear with human splice variant 8A (Figure 3d). In the position equivalent to the exon 9–10 junction in human, there is in mouse clone MD1 an in-frame CAG insertion (encoding an alanine) (Figure 3g). In addition, clone MD1 lacks the human exon equivalents 14 to 16 (Figure 3g). This apparent splicing event of MD1 results in a frameshift of the open reading frame. To determine whether continuity between human exon equivalents 14 to 16 was also present in mouse, we performed PCR using primers to exons 13 and 17 of MD1 on murine testis cDNA, and obtained a single band. Cloning and sequencing revealed that this clone (M1357–1774) contained a splicing product that was completely colinear to the human transcript (Figure 3h). Therefore, we conclude that MD1 represents an aberrantly spliced transcript and that splicing of murine *Nphp1* in this region can occur in a manner colinear to the human transcript. The composite *Nphp1* mouse cDNA comprises 2332 bp. It terminates with a poly(A) stretch, which indicates a full-length 3′ end. The composite murine *Nphp1* cDNA sequence was deposited with GenBank (accession no. AF127180). Sequence identity between human- and mouse-deduced amino acid sequences was 83%, when the human exon splice variant 8A (Figure 3d) was used for comparison.

Identification of a C. Elegans Homologue of NPHP1

Sequence comparison of human and mouse *Nphp1* cDNA yielded high similarity with a putative gene of *C. elegans* (*M28.7*), which has been recently identified by the nematode *C. elegans* genome sequencing project (GenBank accession no. Z49911). Genomic sequence and exon/intron structure for this *C. elegans NPHP1* homologue suggests the presence of nine exons. Exon-intron structure was partially conserved between *NPHP1* genes from mammals (human and mouse) and from *C. elegans* as indicated in Figures 1 and 3. The *C. elegans NPHP1* homologue shows 23% amino acid identity and 42% similarity to the human sequence, after adjustments for gaps.

Identification of Conserved Protein Domains

Nephrocystin is a novel gene product. However, it contains a short segment that is highly similar to known SH3 domains (5,6). To further characterize the amino acid sequence in which the SH3 domain of nephrocystin is embedded, deduced amino acid sequences of human, mouse, and *C. elegans* nephrocystin were compared. Sequence comparison between human and mouse indicated for both E-rich domains, which flank the SH3 domain (see below), two flanking short gaps each (Figure 1). This finding suggests that the exact number of negatively charged residues might not be critical for the function of E-rich domains. An additional gap results from insertion of "CAG" coding for alanine in mouse cDNA clone MD1 at the splice junction from exon 9 to exon 10 (Figure 1 and Figure 3g). After adjustment for these small gaps, there is between human and mouse amino acid sequence 91% similarity and 83% identity, whereas between human nephrocystin and the *C. elegans* nephrocystin-like sequence amino acid sequence similarity is 42% (23% identity) (Figure 1).

Extensive sequence comparison of nephrocystin-deduced amino acid sequence to databases resulted in the identification of putative structural domains as well as segments of significant sequence similarity with known proteins. Exons 1, 2, 3, and 4 in human/mouse and exon 1, 2, and 3 in *C. elegans* encode multiple putative coiled-coil domains (Figures 1, 4, and 5). For their analysis we used the secondary structure prediction program "COILS," which modeled with high probability (score >0.9) three amphipathic α helices, termed I, II, and III for human nephrocystin sequence (Figure 5). The two putative coiled-coils detected in the *C. elegans* nephrocystin homologue correspond to human coiled-coils II and III (data not shown). Coiled-coil domains are amphipathic α-helical structures of heptad repeats, in which hydrophobic amino acids are found in positions 1 and 4 (Figure 5). This structure resembles a cylinder, which on one side in a row slightly oblique to its longitudinal axis exposes hydrophobic amino acid residues (Figures 4 and 5). Two such coiled-coil cylinders may bind to each other by hydrophobic interaction between these residues. The structure resembles two aligned rods, which are slightly intertwined (21).

Besides sequence conservation between human, mouse, and *C. elegans*, the sequence of all three coiled-coil domains of human nephrocystin was found to be conserved in continuity in skeletal muscle myosin, in the region of the myosin S2 seg-

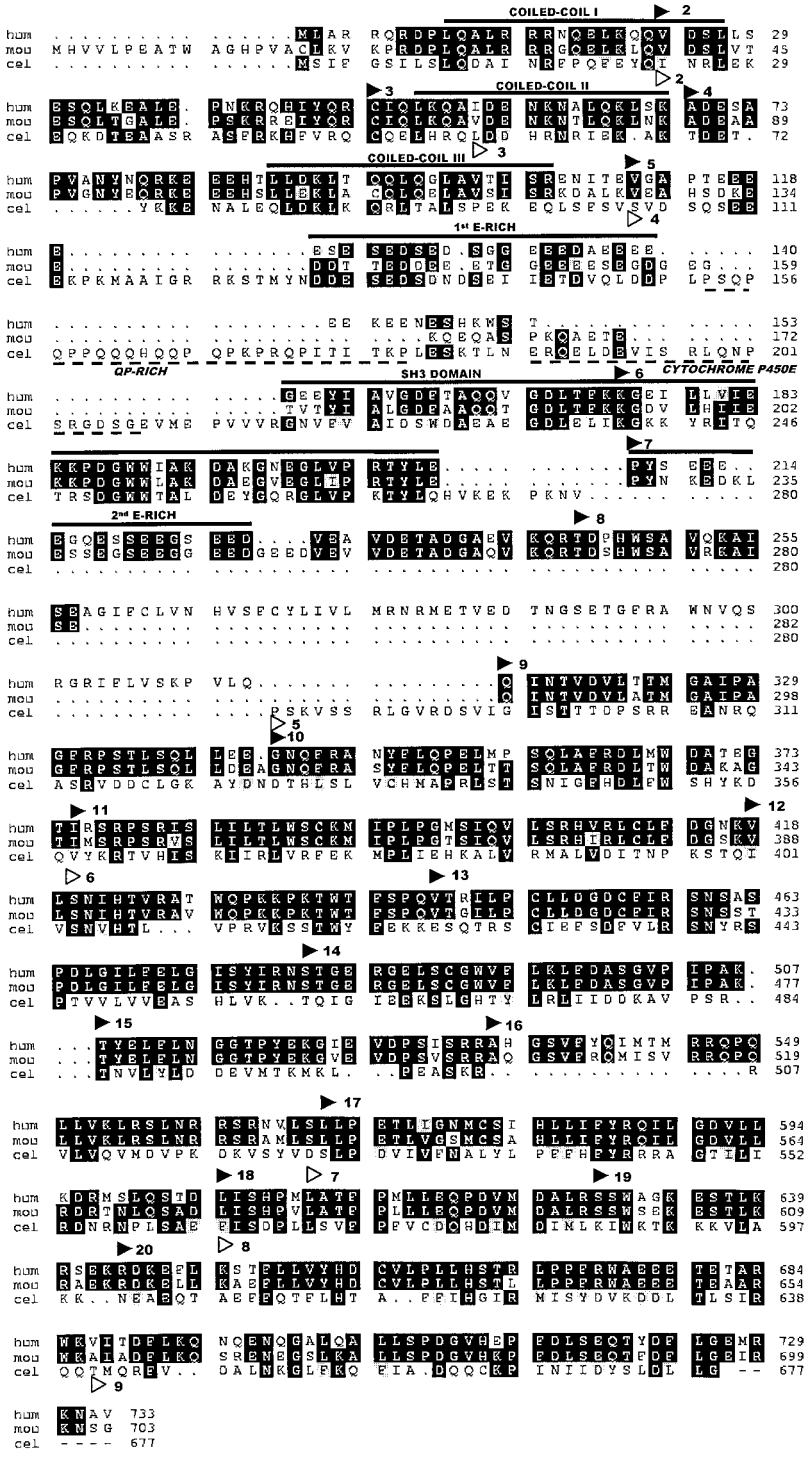

Figure 1. Amino acid sequence alignment of nephrocystin amino acid sequence from human (hum), mouse (mou), and *Caenorhabditis elegans* (*C. elegans*) (cel). Alignments were made with BLAST and PILEUP programs, using standard parameters with minor adjustments by eye. Identical amino acids are shown white on black, and different degrees of sequence conservation are indicated by different shades of gray. Beginnings of exons are shown as filled triangles for human and mouse (inferred) and as open triangles for *C. elegans*. Solid horizontal lines above the alignment indicate segments of putative protein domains or sequence-related segments (>30% identity) identified from databases. For *C. elegans*, these segments are indicated by dashed lines. The following putative domains are indicated (positions of first to last amino acid in human): COILED-COIL I, II, and III: putative coiled-coil domains I (10–27), II (49–68), and III (89–105); 1st E-RICH: first E-rich segment (120–147); SH3: *src*-homology 3 domain (157–208; 50% sequence identity to human *c-crk* oncogene; Swiss-Prot. accession no. P46108); 2nd E-RICH: second E-rich segment (209–227). Segments of putative protein domains of significant sequence similarity to nephrocystin-like sequence of *C. elegans* are indicated by dashed horizontal lines below the alignment. The following domains or similarities are indicated (first to last amino acid; % identity; Swiss-Prot. accession no.): QP-RICH: glutamine/proline-rich domain (153–189). CYTOCHROME P450: sequence similar to cytochrome P450 (197–224; 46% sequence identity; Q29473).

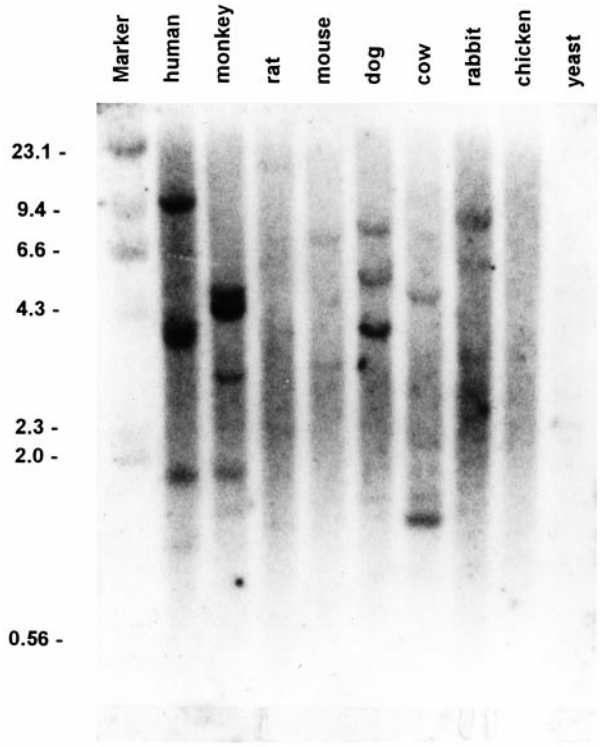

Figure 2. Zoo blot analysis with a human *NPHP1* cDNA. A human Southern blot, containing *Eco*RI-digested genomic DNA of the indicated species, was hybridized at normal stringency with a human *NPHP1* cDNA containing exon 10 to the end of the coding region (nucleotides [nt] 1022–2138) (Figure 3). Size markers in kilobases are shown on the left. Recognition of 1 to 5 bands in most lanes indicates the presence of at least one sequence-related gene in the species examined except chicken and yeast.

ment including the "hinge" region, where a coiled-coil structure is suggested (29% identity, 52% similarity; accession no. P13538). It is also conserved in continuity by many other proteins, which are involved in cytoskeletal scaffolding structures, vesicular traffic, or chromatin binding (list available from the authors).

The nephrocystin SH3 domain, which is highly conserved throughout evolution including yeast (5), is encoded in the human transcript by two exons: the 3′ half of exon 5 and all of exon 6 (Figure 1 and 4). We found that the 5′ half of exon 5 encodes a glutamate-rich (E-rich) sequence (termed first E-rich domain) (Figure 4). This domain contains from the start of exon 5 to the beginning of the SH3 domain 23 negatively charged amino acid residues (E or D) within 43 consecutive amino acids (53%). Even more strikingly, within a core sequence of 26 amino acids, there are 19 glutamate (E) or aspartate (D) residues (83%). In *C. elegans*, an equivalent was found for the first E-rich region with amino acid sequence identity of 11/22 (50%) to the human sequence (Figure 1). This finding indicates that the SH3 domain has been conserved between nematode and mammals within the context of the coiled-coil and first E-rich domain (Figures 1 and 4). At closer inspection, the E-rich domain in *C. elegans* is flanked by short sequences not found in human and mouse (see below), whereas in the two mammals this E-rich domain was in direct continuity with the upstream coiled-coil domain and with the downstream SH3 domain (Figures 1 and 4). Immediately following the SH3 domain, there is in human and mouse a second E-rich domain, which has no equivalent in *C. elegans* (Figures 1 and 4).

In *C. elegans*, the E-rich region and the SH3 domain are separated by two unconserved regions (Figures 1 and 4). The first one was a glutamine/proline (QP)-rich domain and the second one a sequence with high similarity to cytochrome P450 (data not shown). The QP-rich sequence over a stretch of 21 amino acids was highly similar (>40% identity) to sequences containing faithful or incomplete triplet repeats of the sequence "PQQ." The SH3 domain was described previously (5). It had been found to be highly homologous to human and mouse proto-oncogenes *c-crk*. This SH3 domain shows very high amino acid sequence conservation between human and *C. elegans* (60% similarity and 40% identity) (Figures 1 and 4).

From the data on primary and secondary structure predictions for nephrocystin, we conclude that human and mouse nephrocystin encode putative domain structures in the following order (Figure 4): coiled-coil domains I, II, and III, first E-rich domain, SH3 domain, second E-rich domain. In *C. elegans*, this domain structure is conserved with three exceptions: There is no equivalent for coiled-coil I, there is an interspersed QP-rich and a cytochrome P450-like region between the first E-rich and SH3 domains, and there is no second E-rich domain.

Nephrocystin cDNA Expression Analysis

To gain insight into tissue specificity of *NPHP1* expression, extensive Northern, Northern dot blot, and *in situ* hybridization analyses were performed on multiple human and mouse tissues. A normalized human poly(A)$^+$RNA dot blot containing 50 different human tissues was hybridized consecutively with a 3′-specific human *NPHP1* cDNA (exons 9 to 20), and with a 5′-specific human cDNA (exons 1 to 8) (Figure 3). There is widespread tissue expression, with strongest expression in pituitary gland, spinal cord, thyroid gland, testis, skeletal muscle, trachea and kidney, in order of strength (Figure 6a). The 5′-specific probe in addition shows strong expression also in lymph node (Figure 6b). This 5′-specific expression pattern might be the result of differential expression of an alternative short 5′ transcript, which is polyadenylated in exon 8′ as exemplified by EST yy63e10 (Figure 3e). To demonstrate the existence of this alternative transcript, a human multiple tissue Northern blot, which when previously hybridized with the 3′-specific probe yielded a 4.5-kb full-length transcript (5), was now probed with the 5′-specific probe and revealed in fact the presence of a short alternative transcript of 1.2 kb (Figure 7a). To corroborate the *NPHP1* tissue expression pattern in a closely related organism, a murine poly(A)$^+$RNA dot blot containing 22 different murine tissues, including whole mouse embryo of days post coitum 7, 11, 15, and 17, was hybridized with mouse *Nphp1* cDNA clone MD1 (exons 5 to 20 without exons 14 to 16). The pattern observed was similar to results with the 3′-specific probe from human (Figure 6, a and b), with the exception that expression was strongest in mouse testis

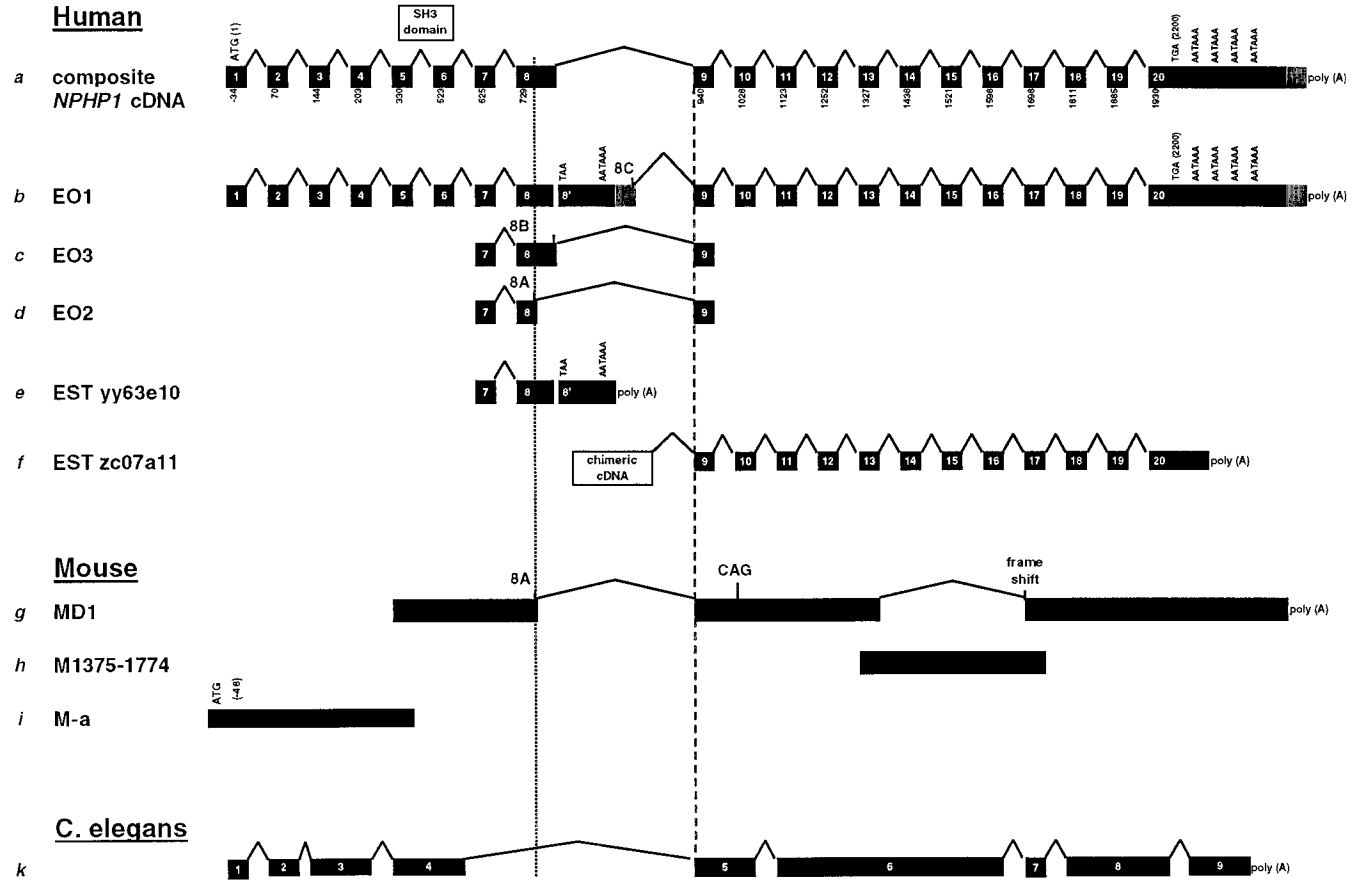

Figure 3. Alternative splice products in *NPHP1* cDNA from human (a through f), mouse (g through i), and *Caenorhabditis elegans* (k). Exons are denoted as black rectangles, numbered in white, and their first nucleotide is given relative to the start of translation (+1) in human. Introns and splicing alternatives are shown as circumflexes. Alu repeat sequences are depicted as grey boxes. A dotted vertical line indicates the position of exon 8 splice variant "8A" (see d), and a dashed vertical line indicates the position of the strong splice acceptor of exon 9. Sequences a through c, e, and f have been reported previously. (a) Composite human *NPHP1* cDNA derived from partial human cDNA (b through f). The position of the sequence encoding the SH3 domain is indicated. Positions of start and stop codons are indicated, as well as four polyadenylation signals (AATAAA) in human, which are differentially used by different transcripts. (b) cDNA clone EO1 most likely represents an incompletely spliced pre-mRNA, since exon 8′, which contains a stop codon (TAA) and a polyadenylation signal (AATAAA), has not been spliced out from the transcript. A consensus splice donor site ("8C") in the first half of an Alu repetitive element is used for splicing onto exon 9. (c) In clone EO3, which represents a reverse transcription (RT)-PCR product between primers to exons 7 and 9 (5), a bona fide splice donor of exon 8 ("8B") is used to skip the stop codon of exon 8′ and splice onto exon 9. Both splice variants (8A and 8B) were also described by Saunier *et al.* (6). (d) Clone EO2, an RT-PCR product of the same reaction as in c, uses the alternative splice donor ("8A"), which is also used by murine clone MD1 (see g) and in an additional transcript isolated from a human testis cDNA library (G. Walz, personal communication). (e) EST yy63e10 represents a short 5′ alternative transcript, which uses the stop codon (TAA) and polyadenylation signal (AATAAA) of exon 8′. (f) EST zc07a11 contains prior to exon 9 a chimeric sequence, which is highly homologous to proteins related to the α_1-macroglobulin family of proteins (5). (g) Murine cDNA clone MD1 was isolated from a mouse diaphragm cDNA library. It is incomplete at its 5′ end and there is an in-frame CAG insertion (coding for an additional alanine) at the exon 9–10 splice junction. This clone is a product of aberrant splicing from exon 13 onto exon 17, which leads to a frameshift. (h) Murine cDNA clone M1357–1774 was produced by PCR using murine testis cDNA and yielded a splicing product colinear in this region to human clone EO1 (b). (i) Murine cDNA clone M-a was produced by 5′ rapid amplification of cDNA ends (RACE), using murine testis cDNA to extend *NPHP1* cDNA sequence toward the 5′ end. k, Genomic structure of the *C. elegans NPHP1*-like cDNA.

(Figure 6c). In addition, this dot blot revealed expression in whole mouse embryo at all developmental stages tested (Figure 6c).

In addition, a multiple tissue murine Northern blot was hybridized with a cDNA probe of mouse *Nphp1* clone MD1 (Figure 3g). A single transcript of 2.4 kb was detected (Figure 7b), which corresponds well with the murine composite full-length sequence of 2332 kb (Figure 3, g through i). This transcript was expressed very weakly in total embryo at most embryonic stages, as well as in fetal and adult kidney and in adult heart even after 3 wk exposure of the blot. In contrast, there is already very strong expression in adult testis detected after an overnight exposure (Figure 7b). This result parallels the results from dot blot analysis in human and mouse (Figure

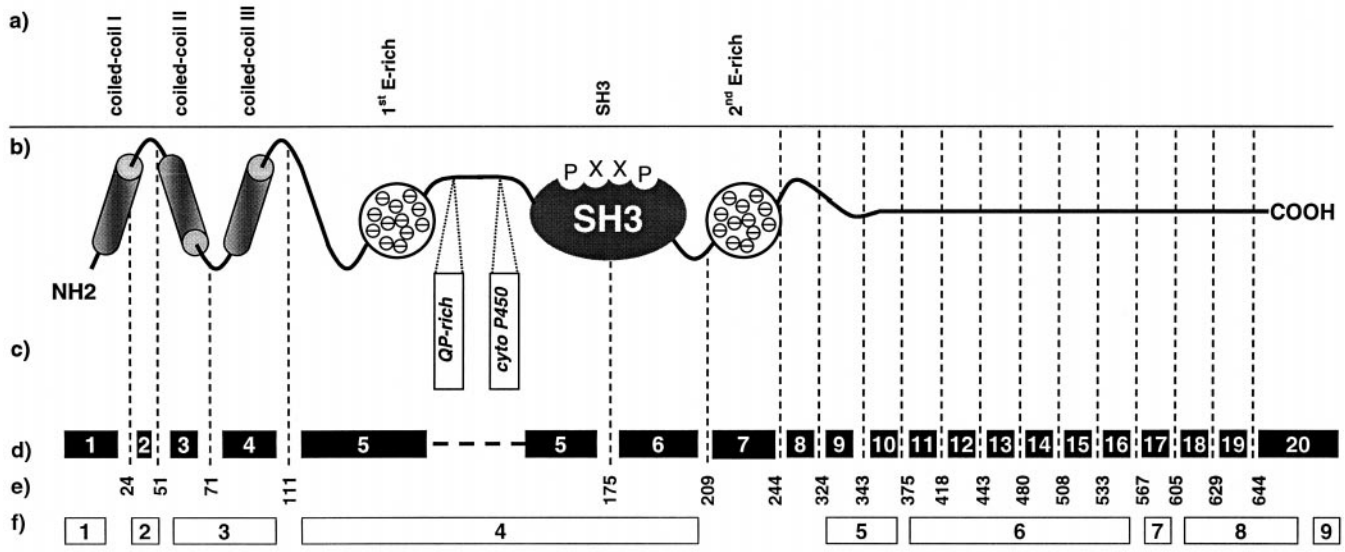

Figure 4. Structural model of nephrocystin. (a) Domains of nephrocystin and sequence-similar segments as derived from database searches (see the section, Identification of Conserved Protein Domains). (b) Graphical representation of putative nephrocystin domain structure. "PXXP" denotes SH3-binding consensus sequence. (c) Additional putative domains in the nephrocystin-like sequence of *C. elegans* are shown in vertical boxes (in italics). In *C. elegans*, there is a QP-rich domain followed by a domain similar to cytochrome P450, inserted between the first E-rich domain and the SH3 domain (see legend to Figure 1 and text). (d) Exon-intron boundaries in human (Figure 3) in relation to putative domain structure in human (connected by vertical dashed lines). (e) Human amino acid sequence numbering (human nephrocystin) (see also Figure 1). (f) Exon-intron boundaries in *C. elegans* in relation to human exon-intron structure in d.

6, a and c), and expression in adult kidney and heart is in agreement with previous Northern analysis in adult human tissues (5).

To evaluate tissue-specific expression during mouse embryonic development, *in situ* hybridization was performed using as a probe murine *Nphp1* cDNA clone MD52-2284 (contains exons 1 to 20 without exons 14 to 16) with whole mouse embryos. Expression was found to be widespread but low between days p.c. 7.5 and 11.5 (Figure 8). Because Northern analysis has shown strong *Nphp1* expression in testis, *in situ* hybridization on testis sections of 6-wk-old mice was performed to gain a cellular resolution of *Nphp1* expression in this tissue. Strong expression was found in seminiferous tubules (Figure 9, a and c). Differential expression for specific cell types was observed, with strong expression in cell stages at or beyond meiosis, such as, spermatocytes I and II (result of first meiotic division), spermatids (result of second meiotic division), and sperm (Figure 9b). In contrast, there was no expression in spermatogonia A and B, Sertoli cells, and interstitial Leydig cells. Likewise, semithin kidney sections of adult and embryonic stages yielded no signal above sense control for *Nphp1* expression, under the conditions used to demonstrate *Nphp1* mRNA expression in the testis.

Discussion

When nephrocystin was first described, the only sequence similarity to known gene products that was recognized was the presence of an SH3 domain (5,6). To learn more about the amino acid sequence context of this SH3 domain, we isolated an *Nphp1* cDNA from mouse and conducted extensive cDNA and amino acid sequence comparison with a nephrocystin-like sequence of *C. elegans*. Amino acid sequence comparisons between human, mouse, and *C. elegans* showed amino acid sequence identity of 83% between human and mouse nephrocystin, and 23% between human and the nephrocystin-like sequence in *C. elegans*. Secondary structure predictions suggest a model in which human and mouse nephrocystin have a putative domain structure in the order from N-terminal to C-terminal (Figure 4): coiled-coil domains I, II, and III, first E-rich domain, SH3 domain, second E-rich domain. In *C. elegans*, this domain structure is conserved with three exceptions: There is no equivalent for coiled-coil I, there is an interspersed QP-rich region and a cytochrome P450-like region between the first E-rich and SH3 domains, and there is no second E-rich domain.

It is interesting to note that in autosomal dominant polycystic kidney disease, the two gene products (polycystin 1 and 2) of the two disease forms strongly interact with each other through coiled-coil domains (22,23). The finding that several domains of protein-protein interaction (SH3 and coiled-coil) are encoded by *NPHP1* suggests that putative binding partners of nephrocystin represent gene products of disease genes of the NPH/MCD complex of diseases.

Regarding potential functions of the putative domains found, one might consider different animal models with an NPH-like phenotype. In this context, three different mouse models of targeted gene disruption of the genes for tensin, angiotensin-converting enzyme (ACE), and Bcl-2 are of interest.

In the tensin knockout mouse model, pathologic changes were only observed in the kidney with a histologic picture highly reminiscent of human NPH: There was marked tubular ectasia and cyst development as well as interstitial inflamma-

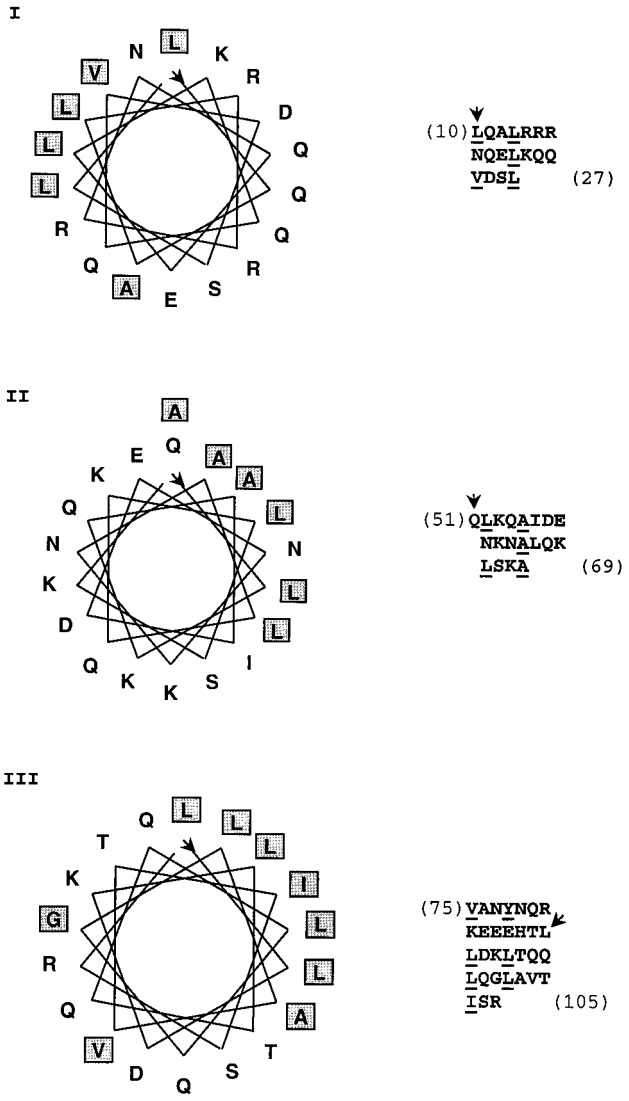

Figure 5. Secondary structure prediction for N-terminal putative coiled-coil domains of nephrocystin. The program COILS, when run for total human nephrocystin sequence, predicted in the N-terminal region three putative amphipathic α helices ("coiled-coils"). In the helical wheel representations of these putative amphipathic α helices I, II, and III shown here, amino acid sequence is plotted clockwise at 80° angles of α-helical peptide bonds, starting at 12 o'clock (arrowhead). Hydrophobic amino acids are shown in gray boxes in single letter coding. To the right of each helical wheel, the amino acid sequence modeled is aligned in heptad repeats. Hydrophobic amino acids are underlined, whenever they occur in positions 1 and 4 of the heptad, and thereby contribute to the amphiphatic periodicity of the putative α helix. The first amino acid used in the helical wheel (at 12 o'clock) is marked by an arrowhead. Amino acid numbering (in parentheses) is according to human nephrocystin sequence (Figure 1). In *C. elegans*, two coiled-coil domains were detected with a window of 21 amino acids. These segments were colinear with putative coiled-coil domains II and III in human (data not shown).

tory infiltration. Electron microscopy demonstrated a lack of focal adhesions in cystic tubules (24). Tensin is an F-actin-binding component of focal adhesions, contains a *src*-homology 2 domain, and plays a central role in focal adhesion signaling. Because most known proteins containing SH3 domains are part of focal adhesion signaling complexes, nephrocystin might also play a role in focal adhesion signaling (25).

There are two additional examples of abnormal expression of focal adhesion components in NPH-like diseases. One comes from studies on integrin expression in human NPH, in which Rahilly and Fleming described strong $\alpha 5\beta 1$ integrin expression in proximal tubules, from which this integrin is normally absent (26). The other comes from the kd/kd mouse model for NPH (27), which was characterized histologically, demonstrating that those proximal tubular cells that were affected by typical lesions showed no expression of fibronectin receptors $\alpha 4\beta 1$ (VLA4) and $\alpha 5\beta 1$ (VLA5), while $\alpha 6\beta 1$ (VLA6) expression was increased (28). In both instances, tubular expression of integrins (as major components of focal adhesion signaling) is altered. The hypothesis that nephrocystin might be part of focal adhesion signaling complexes is also supported in analogy by the finding that coiled-coil-containing proteins are known to be part of cell membrane-attached protein scaffold complexes and focal adhesion signaling complexes. However, this hypothesis will have to be tested by studies on nephrocystin subcellular localization and isolation of protein binding partners.

We found strong similarity between the core E-rich sequences of human and *C. elegans*, with amino acid sequence identity of 11/22. This finding indicates that the SH3 domain has been conserved between nematode and mammals within the context of the coiled-coil and first E-rich domain (Figures 1 and 4). Interestingly, in plectin (P30427), a protein that is known to interact with vimentin and laminin B and that cross-links and anchors intermediate filaments to membranes, there was sequence similarity with all three coiled-coil domains of nephrocystin in continuity with an E-rich sequence (29) (data not shown).

The QP-rich sequences found in the *C. elegans* nephrocystin homologue showed sequence similarity to zyxin, which associates with actin in focal adhesions and may be a component of focal adhesion signal transduction pathways, activating adhesion stimulated changes in gene expression (44% identity; SWISS-PROT accession no. Q15942). In monocytic leukemia zink finger protein, such as in nephrocystin, the QP-rich domain is found in continuity with an N-terminal E-rich domain (43% identity; SWISS-PROT accession no. Q92794).

Knowledge of the presence of these putative structural domains or sequence similarities in nephrocystin can now be used for the generation of functional hypotheses for nephrocystin.

Expression Studies

In nephronophthisis, there is little correlation of the tissue expression pattern of *NPHP1* with the clinical phenotype, which exhibits pathogenic changes only in the kidney (5,6). This is not an unusual situation, however, and has been observed in other monogenic diseases such as X-linked retinitis pigmentosa, in which the *RPGR* gene is widely expressed but detected only in very low levels in the retina, where the only pathogenic changes occur (30).

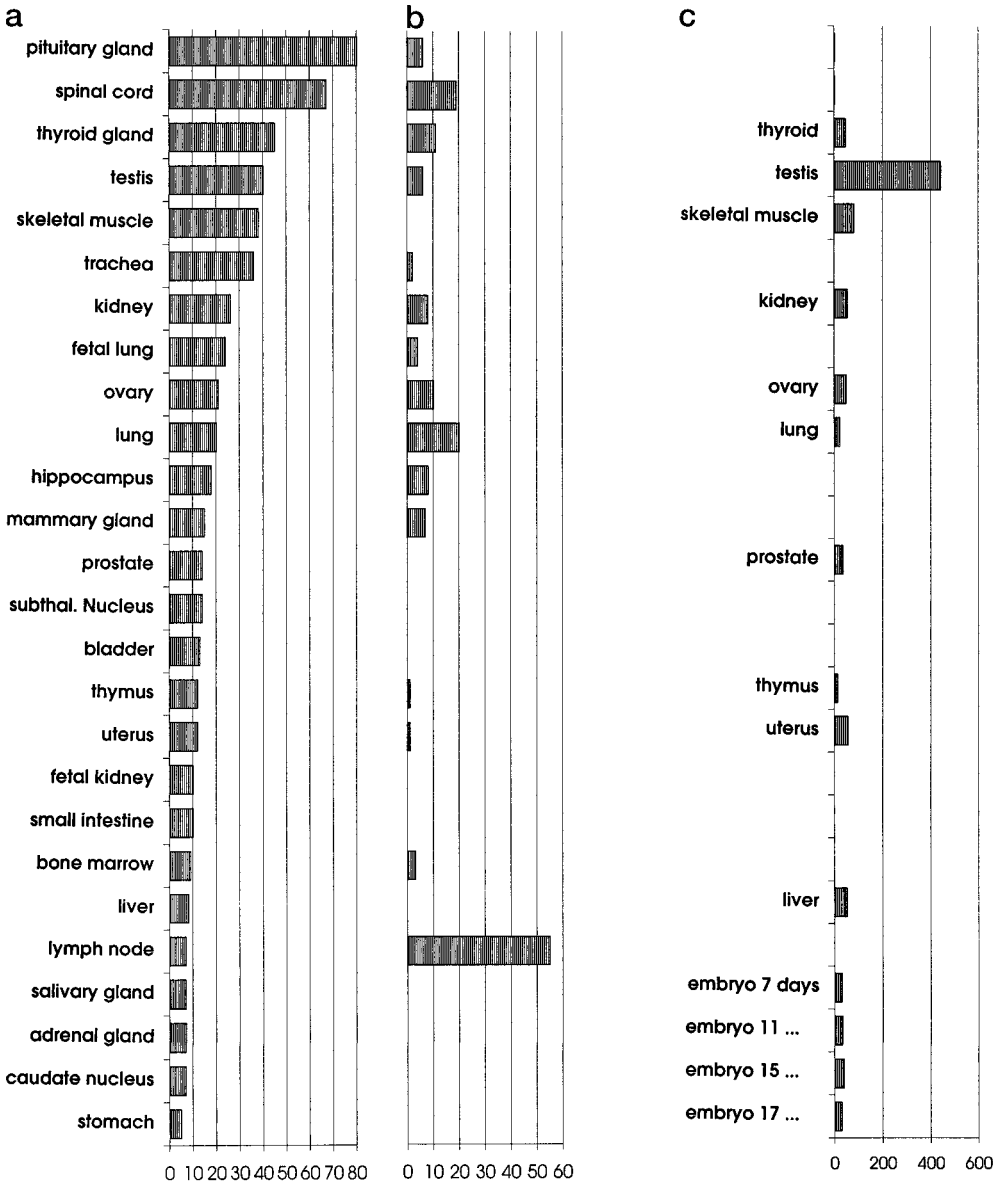

Figure 6. Northern dot blot analysis of tissue-specific mRNA expression in human and murine *Nphp1*. A normalized human poly(A)$^+$RNA blot containing 43 different human adult and seven fetal tissues (a and b), and a murine poly(A)$^+$RNA blot containing 18 murine adult and four fetal tissues (c) were hybridized with *Nphp1* cDNA probes. Only results from tissues giving a signal above background are shown. (a) Hybridization with 3′-specific human *NPHP1* cDNA (nt 1026–2114; contains exons 9 through 20). (b) Hybridization with 5′-specific human cDNA (nt 10–937; contains exons 1 through 8). (c) Hybridization with murine *Nphp1* cDNA clone MD1 (nt 456–2217 in relation to human start codon; contains exons 5 through 20 without 74 to 76). Optical density was normalized against the background signal on yeast and *Escherichia coli* RNA (100 ng) and expressed as relative units. All tissues that yielded a signal are shown and ordered by strength of hybridization for the 3′ human probe (a). Murine tissues are depicted in c on the same line as human tissues with the exception of the last four lines, which display mouse embryonic tissues. Note that there is widespread tissue expression with strongest expression in pituitary gland, spinal cord, thyroid gland, testis, skeletal muscle, trachea, and kidney (a). Expression pattern was similar for all three probes with the following exceptions: In human the 5′-specific human probe detected a strong signal in lymph node (b). In mouse, expression was by far strongest in testis (c).

We found tissue-specific *Nphp1* expression in adult mouse testis, with restriction to distinct cell stages of meiotic or postmeiotic spermatogenesis. This has been described for a few other genes (31). As an example, cyclin A1 is expressed in mice exclusively in the germ cell lineage, and in testis in cell stages immediately preceding meiosis and thereafter (32,33). This expression pattern is highly reminiscent of *Nphp1* expression in mouse testis. It is interesting to note that in cyclin A1 knockout mice (34), spermatocytes undergo apoptotic cell death, resulting in infertility of male cyclin A1−/− mice. However, current data available to us on 23 male patients with molecular genetically proven NPH1 do not allow assessment of

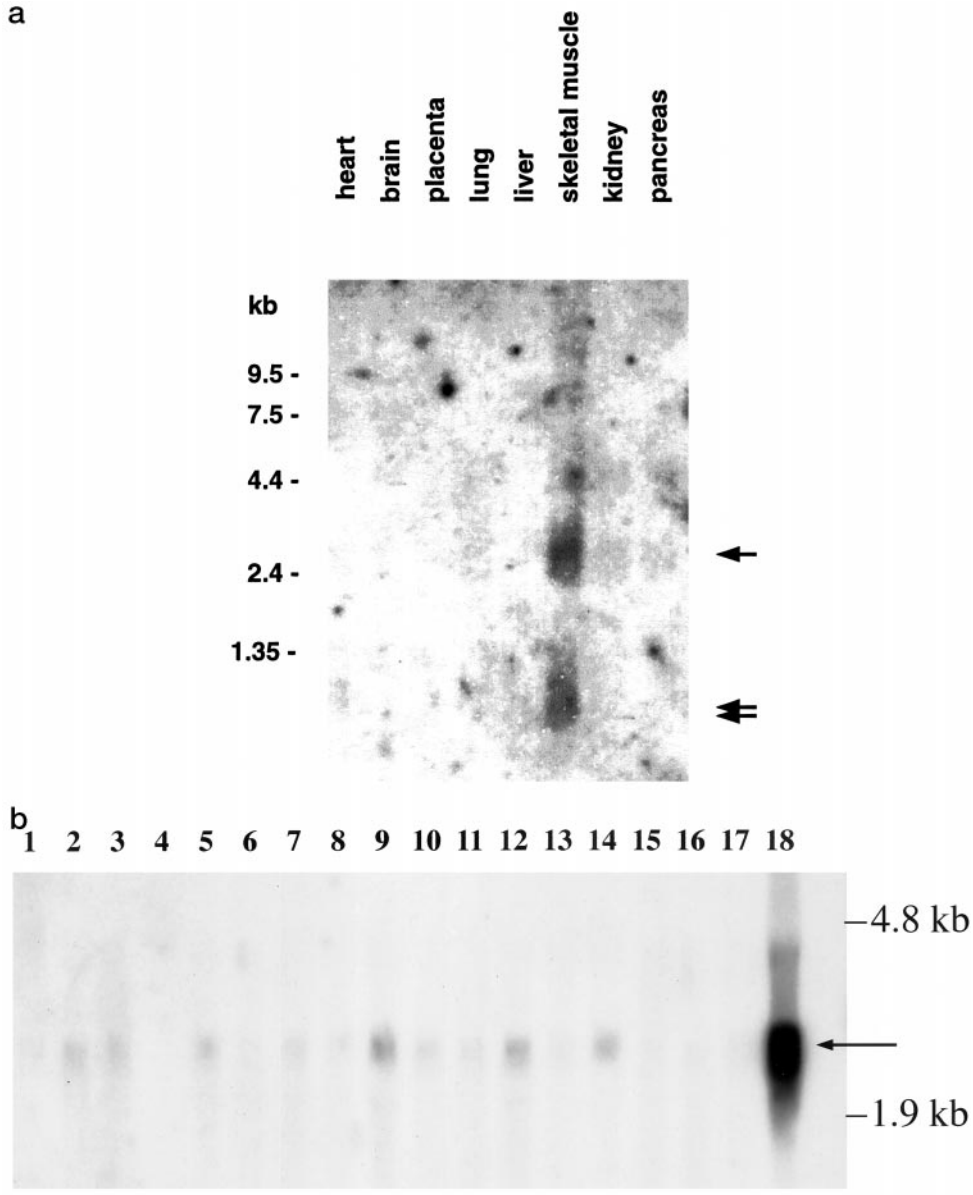

Figure 7. (a) Northern blot analysis of differential *NPHP1* expression of a short alternative 5′ transcript. A multiple tissue Northern blot with human adult poly(A)$^+$RNA was hybridized with a 5′-specific human cDNA probe (nt 10–937), which contains exons 1 through 8 only. This probe detected the same bands that were detected previously by the 3′-specific probe (5). These were the full-length transcript at 4.5 kb and multiple bands in the range 2.4 to 3 kb (single arrow), which are most likely due to usage of alternative polyadenylation sites (5). In addition, however, a band of 1.2 kb was detected in skeletal muscle and weakly in kidney (double arrow). This most likely represents a short 5′ alternative transcript, which is polyadenylated after exon 8 as represented by EST yy63e10 (Figure 2e). Background is strong due to extremely weak expression. A β-actin control of this blot has been published previously (5) and showed equal loading for poly(A)$^+$RNA. (b) Northern blot analysis of total mouse embryo and murine adult tissues. A multiple tissue Northern blot of murine total RNA was hybridized with cDNA of mouse *Nphp1* clone MD1 (Figure 2g). Twenty micrograms of total RNA was loaded into lanes 1 through 8 from total mouse embryo of days post coitum 11.5, 12.5, 13.5, 14.5, 15.5, 16.5, 17.5, and 18.5, respectively. Lanes 9 through 11 are from kidney 18.5 day post coitum, 10 d adult, and 20 d adult, respectively. Lanes 12 through 18 are from adult kidney, brain, heart, liver, lung, muscle, and testis, respectively. Exposure was 3 wk. Note that a transcript of 2.4 kb (arrow) is expressed very weakly in total embryo at most embryonic stages as well as in fetal (lane 9) and adult kidney (lanes 10 through 12) and in adult heart (lane 14). In contrast, there was very strong expression in adult testis. Control hybridization using a *GAPDH* probe indicated equal loading of RNA in each lane (data not shown).

male fertility in human NPH1, due to the relatively young age of NPH1 patients that have received a renal allograft.

In this regard, the mouse model of targeted disruption of the *bcl-2* gene might be of relevance. This mouse model exhibits a renal phenotype similar to NPH, although fulminant apoptosis is present and typical basement membrane changes of NPH are lacking. Because Bcl-2 is a modulator of apoptosis, there might be a link of nephrocystin function to processes of apoptosis in

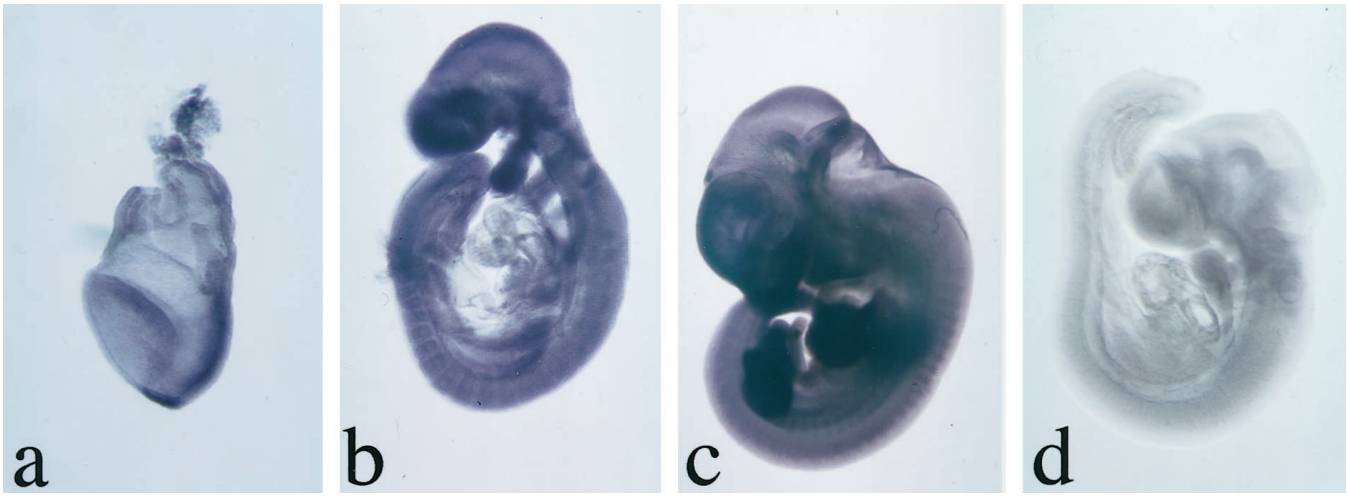

Figure 8. In situ hybridization study of *Nphp1* expression during mouse embryonic development. Antisense *Nphp1* RNA from murine cDNA MD52–2284 was hybridized at days p.c. 7.5 (a), 9.5 (b), and 11.5 (c). Sense control at day p.c. 9.5 is shown in d. Note that expression is widespread and uniform at all stages. A similar result was obtained for stages 8.5 and 10.5 (data not shown). Apparent differences in staining intensity are due to superposition of signal in limb buds and branchial arches.

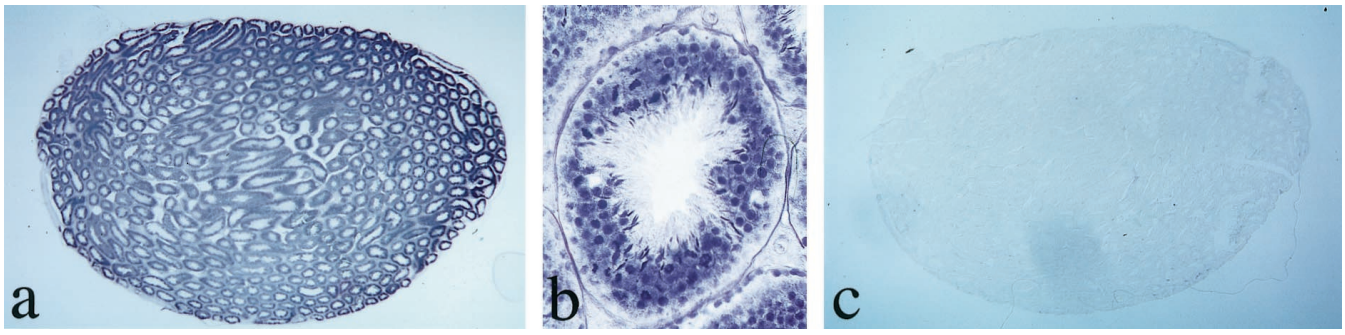

Figure 9. In situ hybridization analysis of *Nphp1* expression in mouse adult testis RNA. Antisense *Nphp1* RNA from murine cDNA MD52–2284 was hybridized to tissue sections of murine adult testis. (a) Total adult testis. (b) Higher magnification showing one seminiferous tubule. (c) Sense control on total adult testis. Note that in b differential expression for different cell types of testis can be observed as follows (in order from the basal lamina inward): lack of expression in spermatogonia A and B and Sertoli cells (all attached to basal lamina); strong expression in cell stages at or beyond meiosis, like spermatocytes I and II, spermatids, and sperm. Leydig cells (in interstitial triangles between tubules) also showed no *Nphp1* expression.

renal tubular cells (35). In this light it seems interesting that Lin *et al.* were able to show in Madin-Darby canine kidney cells, which regularly develop into simple epithelial cell cysts when cultured in type I collagen gel, that *Bcl-2* overexpression averts cyst cavitation (36). Their data indicate that apoptosis may be an essential initial event for renal cyst formation.

Another animal model with an NPH-like phenotype is the knockout mouse for the ACE gene. A testis-specific isoform of this gene transcribed from a promoter within intron 12 is encoded by the 3′ region of the gene and is expressed only in testis. Like nephrocystin in adult mouse, it is specifically expressed in postmeiotic spermatogenic cells and sperm (37). ACE knockout mice show reduced fertility in the male and are phenotypically affected by a nephronophthisis-like disease, with renal medullary cysts, corticotubular atrophy, interstitial inflammation, water wasting, and uremia (38). In addition, there is renal vessel wall hypertrophy together with architectural disruption of the renal vascular tree (39). Vessel wall hypertrophy is also seen in human NPH. Furthermore, ACE is known to play a major role in kidney morphogenesis (40). Interestingly, when ACE knockout mice were interbred with transgenic mice specifically expressing ACE from an artificial testis-specific promoter, fertility in males was restored, but mice maintained kidney defects of ACE−/− mice (41). Thus, the testis-specific form of the ACE gene, like the *Nphp1* gene, is very specifically expressed in meiotic and postmeiotic cells of spermatogenesis, besides weak expression in kidney and other tissues.

It is interesting to note that a nephronophthisis-like phenotype can be produced by targeted disruption of several different genes, since for human diseases of the NPH/MCD complex at least four different recessive and three different dominant gene

loci are known. Isolation of protein-protein binding partners of nephrocystin might therefore lead to the identification of disease genes for other diseases of the NPH/MCD complex.

Acknowledgments

Dr. Hildebrandt was supported by a grant from the German Research Foundation (Deutsche Forschungsgemeinschaft Hi 381/3-3). Drs. Hildebrandt and Otto were supported by the Zentrum Klinische Forschung I (ZKF-A1) of Freiburg University (Baden-Württemberg). The excellent technical assistance of Anita Imm and Bénédicte Haenig is gratefully acknowledged. We thank Ch. Peters and K. Geiger for help with cDNA sequencing.

References

1. Hildebrandt F: Nephronophthisis. In: *Pediatric Nephrology*, edited by Avner ED, Barratt TM, Harmon W, Baltimore, Lippincott Williams & Wilkins, 1999, pp 453–458
2. Hildebrandt F, Jungers P, Grünfeld JP: Medullary cystic and medullary sponge renal disorders. In: *Diseases of the Kidney*, edited by Schrier WB, Gottschalk C, Boston, Little, Brown and Co., 1996, pp 499–520
3. Kleinknecht C: The inheritance of nephronophthisis. In: *Inheritance of Kidney Diseases*, edited by Spitzer A, Avner ED, Boston, Kluwer Academic Publishers, 1989, pp 277–294
4. Waldherr R, Lennert T, Weber HP, Fodisch HJ, Scharer K: The nephronophthisis complex: A clinicopathologic study in children. *Virchows Arch A Pathol Anat Histol* 394: 235–254, 1982
5. Hildebrandt F, Otto E, Rensing C, Nothwang HG, Vollmer M, Adolphs J, Hanusch H, Brandis M: A novel gene encoding an SH3 domain protein is mutated in nephronophthisis type 1. *Nat Genet* 17: 149–153, 1997
6. Saunier S, Calado J, Heilig R, Silbermann F, Benessy F, Morin G, Konrad M, Broyer M, Gubler MC, Weissenbach J, Antignac C: A novel gene that encodes a protein with a putative src homology 3 domain is a candidate gene for familial juvenile nephronophthisis. *Hum Mol Genet* 6: 2317–2323, 1997
7. Haider NB, Carmi R, Shalev H, Sheffield VC, Landau D: A bedouin kindred with infantile nephronophthisis demonstrates linkage to chromosome 9 by homozygosity mapping. *Am J Hum Genet* 63: 1404–1410, 1998
8. Loken A, Hanssen O, Halvorsen S, Jolster N: Hereditary renal dysplasia and blindness. *Acta Paediatr* 50: 177–184, 1961
9. Senior B, Friedmann A, Braudo J: Juvenile familial nephropathy with tapetoretinal degeneration: A new oculorenal dystrophy. *Am J Ophthal* 52: 625–633, 1961
10. Saunier S, Morin G, Calado J, Benessy F, Silbermann F, Antignac C: Large deletions of the NPH1 region in Cogan syndrome (CS) associated with familial juvenile nephronophthisis (NPH) [Abstract]. *Am J Hum Genet* 61: A346, 1997
11. Gardner KDJ: Evolution of clinical signs in adult-onset cystic disease of the renal medulla. *Ann Intern Med* 74: 47–54, 1971
12. Christodoulou K, Tsingis M, Stavrou C, Eleftheriou A, Papapavlou P, Patsalis PC, Ioannou P, Pierides A, Constantinou DC: Chromosome 1 localization of a gene for autosomal dominant medullary cystic kidney disease. *Hum Mol Genet* 7: 905–911, 1998
13. Scolari F, Ghiggeri GM, Amoroso A, Caridi GL, Aridon P: Genetic heterogeneity for autosomal dominant medullary cystic kidney disease (ADMCKD) [Abstract]. *J Am Soc Nephrol* 9: 393A, 1998
14. Clark EA, Brugge JS: Integrins and signal transduction pathways: The road taken. *Science* 268: 233–239, 1995
15. Defilippi P, Gismondi A, Santoni A, Tarone G: *Signal Transduction by Integrins*, New York, Springer, 1997
16. Sambrook J, Fritsch EF, Maniatis T: *Molecular Cloning: A Laboratory Manual*, Cold Spring Harbor, NY, Cold Spring Harbor Laboratory Press, 1989
17. Burk O, Mink S, Ringwald M, Klempnauer KH: Synergistic activation of the chicken mim-1 gene by v-myb and C/EBP transcription factors. *EMBO J* 12: 2027–2038, 1993
18. Parr BA, Shea MJ, Vassileva G, McMahon AP: Mouse Wnt genes exhibit discrete domains of expression in the early embryonic CNS and limb buds. *Development* 119: 247–261, 1993
19. Knecht AK, Good PJ, Dawid IB, Harland RM: Dorsal-ventral patterning and differentiation of noggin-induced neural tissue in the absence of mesoderm. *Development* 121: 1927–1935, 1995
20. Lescher B, Haenig B, Kispert A: sFRP-2 is a target of the Wnt-4 signaling pathway in the developing metanephric kidney [In Process Citation]. *Dev Dyn* 213: 440–451, 1998
21. Lodish H, Baltimore D, Berk A, Zipursky SL, Matsudaira P, Darnell J: *Molecular Cell Biology*, New York, W. H. Freeman and Co., 1995
22. Qian F, Germino FJ, Cai Y, Zhang X, Somlo S, Germino GG: PKD1 interacts with PKD2 through a probable coiled-coil domain. *Nat Genet* 16: 179–183, 1997
23. Tsiokas L, Kim E, Arnould T, Sukhatme VP, Walz G: Homo- and heterodimeric interactions between the gene products of PKD1 and PKD2. *Proc Natl Acad Sci USA* 94: 6965–6970, 1997
24. Lo SH, Yu QC, Degenstein L, Chen LB, Fuchs E: Progressive kidney degeneration in mice lacking tensin. *J Cell Biol* 136: 1349–1361, 1997
25. Hildebrandt F: Identification of a gene for nephronophthisis. *Nephrol Dial Transplant* 13: 1334–1336, 1998
26. Rahilly MA, Fleming S: Abnormal integrin receptor expression in two cases of familial nephronophthisis. *Histopathology* 26: 345–349, 1995
27. Lyon MF, Hulse EV: An inherited kidney disease of mice resembling human nephronophthisis. *J Med Genet* 8: 41–48, 1971
28. Sibalic V, Sun L, Sibalic A, Oertli B, Ritthaler T, Wuthrich RP: Characteristic matrix and tubular basement membrane abnormalities in the CBA/Ca-kdkd mouse model of hereditary tubulointerstitial disease. *Nephron* 80: 305–313, 1998
29. Liu CG, Maercker C, Castanon MJ Hauptmann R, Wiche G: Human plectin: Organization of the gene, sequence analysis, and chromosome localization (8q24). *Proc Natl Acad Sci USA* 93: 4278–4283, 1996
30. Meindl A, Dry K, Herrmann K, Manson F, Ciccodicola A, Edgar A, Carvalho MR, Achatz H, Hellebrand H, Lennon A, Migliaccio C, Porter K, Zrenner E, Bird A, Jay M, Lorenz B, Wittwer B, D'Urso M, Meitinger T, Wright A: A gene (RPGR) with homology to the RCC1 guanine nucleotide exchange factor is mutated in X-linked retinitis pigmentosa (RP3). *Nat Genet* 13: 35–42, 1996
31. Eddy EM: Regulation of gene expression during spermatogenesis. *Semin Cell Dev Biol* 9: 451–457, 1998
32. Sweeney C, Murphy M, Kubelka M, Ravnik SE, Hawkins CF, Wolgemuth DJ, Carrington M: A distinct cyclin A is expressed in germ cells in the mouse. *Development* 122: 53–64, 1996
33. Wu S, Wolgemuth DJ: The distinct and developmentally regulated patterns of expression of members of the mouse Cdc25 gene family suggest differential functions during gametogenesis. *Dev Biol* 170: 195–206, 1995

34. Liu D, Matzuk MM, Sung WK, Guo Q, Wang P, Wolgemuth DJ: Cyclin A1 is required for meiosis in the male mouse. *Nat Genet* 20: 377–380, 1998
35. Veis DJ, Sorenson CM, Shutter JR, Korsmeyer SJ: Bcl-2-deficient mice demonstrate fulminant lymphoid apoptosis, polycystic kidneys, and hypopigmented hair. *Cell* 75: 229–240, 1993
36. Lin HH, Yang TP, Jiang ST, Yang HY, Tang MJ: Bcl-2 overexpression prevents apoptosis-induced Madin-Darby canine kidney simple epithelial cyst formation. *Kidney Int* 55: 168–178, 1999
37. Krege JH, John SW, Langenbach LL, Hodgin JB, Hagaman JR, Bachman ES, Jennette JC, O'Brien DA, Smithies O: Male-female differences in fertility and blood pressure in ACE-deficient mice. *Nature* 375: 146–148, 1995
38. Carpenter C, Honkanen AA, Mashimo H, Goss KA, Huang P, Fishman MC, Asaad M, Dorso CR, Cheung H: Renal abnormalities in mutant mice [Letter]. *Nature* 380: 292, 1996
39. Hilgers KF, Reddi V, Krege JH, Smithies O, Gomez RA: Aberrant renal vascular morphology and renin expression in mutant mice lacking angiotensin-converting enzyme. *Hypertension* 29: 216–221, 1997
40. Gomez RA: Role of angiotensin in renal vascular development. *Kidney Int Suppl* 67: S12–S16, 1998
41. Ramaraj P, Kessler SP, Colmenares C, Sen GC: Selective restoration of male fertility in mice lacking angiotensin-converting enzyme by sperm-specific expression of the testicular isozyme. *J Clin Invest* 102: 371–378, 1998